BBA 41830

Electron transfer in reaction centers of *Rhodopseudomonas sphaeroides*. II. Free energy and kinetic relations between the acceptor states $Q_A^- Q_B^-$ and $Q_A Q_B^{2-}$
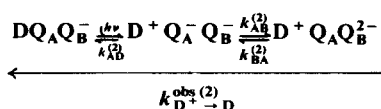
D. Kleinfeld *, M.Y. Okamura and G. Feher **

Department of Physics, University of California at San Diego, La Jolla, CA 92093 (U.S.A.)

Thermodynamic equilibria and electron transfer kinetics involving the quinone acceptor complex in reaction centers from *Rhodopseudomonas sphaeroides* were investigated. We focussed on reactions involving the two-electron states $Q_A^- Q_B^-$ and $Q_A Q_B^{2-}$, described by the scheme

$$DQ_AQ_B^- \underset{k_{AD}^{(2)}}{\overset{h\nu}{\rightleftharpoons}} D^+ Q_A^- Q_B^- \underset{k_{BA}^{(2)}}{\overset{k_{AB}^{(2)}}{\rightleftharpoons}} D^+ Q_A Q_B^{2-}$$

$$\xleftarrow{\hspace{4cm}}$$
$$k_{D^+ \to D}^{obs\,(2)}$$

The equilibrium partitioning between $Q_A^- Q_B^-$ and $Q_A Q_B^{2-}$ was determined spectroscopically from either the concentration of oxidized cytochrome c or the concentration of semiquinone after successive flashes of light. At pH < 9.5, $Q_A Q_B^{2-}$ is stabilized relative to $Q_A^- Q_B^-$, while for pH > 9.5, $Q_A^- Q_B^-$ is energetically favored. The reduction of Q_A, to form $Q_A^- Q_B^-$, is not associated with a protonation step (pK < 8). However, the reduction of Q_B^-, to form the final state $Q_A Q_B^{2-}$, is accompanied by an uptake of a proton (p$K \geqslant 10.7$). The preferential interaction of a proton with $Q_A Q_B^{2-}$ provides the driving force for the forward electron transfer. The shift toward the photochemically inactive state $Q_A^- Q_B^-$ with increasing pH may serve as a feedback mechanism in photosynthetic organisms to limit the rise in intracellular pH. The electron-transfer rate constants were determined from the observed kinetics and the equilibria between the states $Q_A Q_B^{2-}$ and $Q_A^- Q_B^-$. The forward rate constant $k_{AB}^{(2)}$ was approximately proportional to the proton concentration, whereas $k_{BA}^{(2)}$ depended only weakly on pH. The recombination kinetics of $D^+ Q_A Q_B^{2-}$ was biphasic. The slow rate agreed with the predicted charge recombination via the intermediate state $D^+ Q_A^- Q_B^-$; the fast rate may be due to the recombination from a separate (conformational) state. The results of this work were combined with those of a previous study on reactions involving the one-electron precursor states $Q_A^- Q_B$ and $Q_A Q_B^-$ (Kleinfeld, D., Okamura, M.Y., and Feher, G. (1984) Biochim. Biophys. Acta 766, 126–140). The overall sequence for the protonation of the reaction center in response to successive reductions of the acceptor complex involves the uptake of one proton for each electron transferred to Q_B. This sequential uptake initiates the formation of a proton gradient across the cell membrane.

---

* Present address: Department of Molecular Biophysics, AT
&T Bell Laboratories, Murray Hill, NJ 07974, U.S.A.
** To whom reprint requests should be addressed.
Abbreviations: Caps, 3-(cyclohexylamino)-1-propanesulfonic acid; Ches, cyclohexylaminoethanesulfonic acid; DAD, 2,3,5,6-tetramethyl-*p*-phenylenediamine; DMF, dimethyl for- mamide; EtOH, ethanol; LDAO, lauryldimethylamine N-oxide; MeOH, methanol; Mes, 4-morpholineethanesulfonic acid; *o*-phen, 1,10-phenanthroline; Pipes, 1,4-piperazinediethane-sulfonic acid; U-Q-10, 2,3-dimethoxy-5-methyl-6-de-caisoprenyl-*p*-benzoquinone; Cyt, cytochrome; RC, Reaction center.

Introduction

The process of photosynthesis begins in the reaction center, a protein-pigment complex that spans the plasma membrane. Reaction centers act as energy transducers, absorbing light and converting it into electrochemical energy through the creation of oxidized and reduced molecules (for review, see Ref. 1). These molecules provide the subsequent driving force for the transport of protons across the membrane. The light-induced electron transfer thus results in the formation of a transmembrane proton gradient whose energy is used for the formation of ATP (for review, see Ref. 2).

Reaction centers from photosynthetic bacteria consist of three polypeptides and a number of cofactors associated with the electron-transfer chain (for reviews, see Refs. 3–5). In this work we focus on a subsystem of the transfer chain consisting of the primary donor, D (a bacteriochlorophyl dimer), and the primary and secondary quinone acceptors, Q_A and Q_B respectively. This subsystem is coupled to exogenous (quinone) acceptors that initiate the transport of protons across the membrane (Refs. 6–8, see also the review in Ref. 9).

In a previous report [10] we examined the free energy and kinetic relations associated with the states formed after the transfer of the first electron to the quinone acceptors. We found that near neutral pH the state $Q_A Q_B^-$ is stabilized relative to $Q_A^- Q_B$, while at high pH $Q_A^- Q_B$ is energetically favorable. Both Q_A^- and Q_B^- associate with a proton, with pK values of 9.8 and 11.3, respectively. The stronger interaction of the proton with Q_B^- provides the driving force for the forward transfer of the electron.

In this work we examine the free energy and kinetic relations associated with the states formed after the transfer of the second electron to the quinone acceptor complex. The equilibrium involved in this system is described by *

$$Q_A^- Q_B^- \underset{k_{BA}^{(2)}}{\overset{k_{AB}^{(2)}}{\rightleftharpoons}} Q_A Q_B^{2-} , \tag{1}$$

---

* For simplicity, the various reaction center states are written unprotonated (see also Eqns. 2–4, 7, 8, 19 and 22). However, they are meant to include the protonated states as well. The topic of protonation is discussed in a later section.
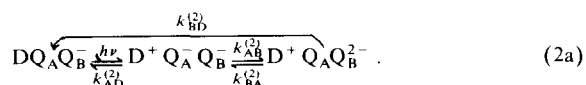
where the superscript (2) indicates that we are concerned with the second electron.

The equilibrium partitioning between $Q_A^- Q_B^-$ and $Q_A Q_B^{2-}$ was determined by using two different assays. In the first, the fraction, β, of reaction centers in the state $Q_A^- Q_B^-$ was determined from the amount of cytochrome c oxidized by D^+ after successive flashes of light. In the second assay, β was obtained from the steady-state semiquinone (i.e., Q_A^- or Q_B^-) absorption after successive flashes. Both assays were performed over a wide pH range.

The electron transfer rate between $Q_A^- Q_B^-$ and $Q_A Q_B^{2-}$, given by $k_{AB}^{(2)} + k_{BA}^{(2)}$, was determined by optically monitoring the decay kinetics of $Q_A^- Q_B^-$ following a flash. In addition, the initial amplitude of this transient signal was used to confirm the pH dependence of β found with the methods outlined above.

The free energy difference ($\Delta G_{obs\ (2)}^0$) between $Q_A^- Q_B^-$ and $Q_A Q_B^{2-}$ was obtained from the partition coefficient β. By combining the experimental results for $k_{AB}^{(2)} + k_{BA}^{(2)}$ with the values of $\Delta G_{obs\ (2)}^0$, the pH dependence of the individual electron-transfer rates $k_{AB}^{(2)}$ and $k_{BA}^{(2)}$ were obtained. From the pH dependence of $\Delta G_{obs\ (2)}^0$ and the individual transfer rates, the protonation steps associated with the formation of $Q_A^- Q_B^-$ and $Q_A Q_B^{2-}$ were deduced. The results of the present study were combined with previous work [10] on the equilibrium between $Q_A^- Q_B$ and $Q_A Q_B^-$ to formulate a model describing how protons are sequentially coupled to the electron-transport chain.

We also examined the charge recombination kinetics of the state $D^+ Q_A Q_B^{2-}$, i.e., the recombination of one of the electrons on Q_B^{2-} with D^+. The electron-transfer scheme describing this process is given by

$$DQ_A^- Q_B^- \underset{k_{AD}^{(2)}}{\overset{h\nu}{\rightleftharpoons}} D^+ Q_A^- Q_B^- \underset{k_{BA}^{(2)}}{\overset{k_{AB}^{(2)}}{\rightleftharpoons}} D^+ Q_A Q_B^{2-} . \tag{2a}$$

The charge recombination can proceed either directly, or indirectly via the intermediate state $D^+ Q_A^- Q_B^-$. When the electron-transfer rate between $Q_A^- Q_B^-$ and $Q_A Q_B^{2-}$ is rapid compared to the recombination rates $k_{AD}^{(2)}$ and $k_{BD}^{(2)}$, the observed recombination rate, $k_{D^+ \to D}^{obs,\ (2)}$, can be ex-

pressed as [10]:

$$k_{D^+ \to D}^{obs\ (2)} = k_{indirect} + k_{direct} = \beta k_{AD}^{(2)} + (1 - \beta) k_{BD}^{(2)} \qquad (2b)$$

where β is the fraction of reaction centers in the state $Q_A^- Q_B^-$. The basis of the method to determine the pathway was to compare the product $\beta k_{AD}^{(2)}$ with $k_{D^+ \to D}^{obs\ (2)}$. From the discrepancy between the value of $k_{D^+ \to D}^{obs\ (2)}$ and $\beta k_{AD}^{(2)}$ the contribution of the direct recombination rate, $k_{BD}^{(2)}$, can be obtained.

Preliminary accounts of this work have been presented [11].

Materials and Methods

Reagents

Cytochrome c(Cyt c) (horse heart type VI, Sigma) was reduced (> 98%) by sodium dithionite (Matheson, Coleman and Bell) and purified on a Sephadex G-200 (Pharmacia) gel filtration column. The concentration of cytochrome was determined from the optical absorption using the extinction coefficient $\epsilon_{red}^{550} = 27.6$ mM$^{-1} \cdot$ cm^{-1} [12]. Solutions of diaminodurene (DAD; 2,3,5,6-tetramethyl-p-phenylenediamine) (Aldrich) and 1,10-phenanthroline (o-phen) (Baker) were prepared in ethanol prior to use.

Reaction centers

Reaction centers were isolated from *R. sphaeroides* R-26 as described [3]. Reaction center concentrations were determined from the optical absorption $A_{1\ cm}^{302}$ and the extinction coefficient $\epsilon^{802} = 288$ mM$^{-1} \cdot$ cm^{-1} [13]. The quinone content was determined by a cytochrome c photooxidation assay and by an assay based on the donor recovery kinetics after a laser flash [14]. Preparations contained slightly less than two quinones per reaction center; the deviation from 2.00, defined as δ, was typically 0.05 ± 0.02. Since the binding of Q_B is substantially weaker than the binding of Q_A(see, e.g., Ref. 14), δ corresponds to the fraction of reaction centers that lack Q_B.

Buffers

All experiments were carried out at 21.5°C in 10 mM buffer and 0.025% (w/v) LDAO with potassium chloride added as required to set the ionic strength at 10 mM. The following pH buffers were used: Mes (Calbiochem-Behring), pH $\leqslant 6.4$; Pipes (Sigma), pH 6.4–7.6; Tris (Schwartz/Mann), pH 7.6–9.0; Ches (Calbiochem-Behring), pH

9.0–10.0; Caps (Calbiochem-Behring), pH $\geqslant 10.0$.

Optical measurements

Optical absorption spectra were recorded with a Cary 17D spectrophotometer (Varian). Flash-induced charge separation was accomplished with a pulsed dye laser ($\lambda_0 = 584$ nm, 0.4 μs pulse width, 0.2 J per pulse) (Phase R). Rapid changes in the optical absorption spectrum following a flash were recorded with a spectrophotometer of local design that had a time resolution of 0.5 μs [10]. The spectral bandwidth in all measurements was less than 1 nm. To limit the exposure of samples to light prior to a flash, the monitoring beam of the spectrophotometer was gated shut until approx. 1 s before the flash. The analysis of data was performed as described [10].

Theoretical models

Reaction center states and cytochrome oxidation after successive flashes

In the presence of an exogenous electron donor (e.g., Cyt c^{2+}), D^+ is reduced and electrons are trapped on the quinone acceptors. The different states ($Q_A Q_B$, $Q_A^- Q_B$, $Q_A Q_B^-$, $Q_A^- Q_B^-$, $Q_A Q_B^{2-}$ and $Q_A^- Q_B^{2-}$) produced after successive flashes are shown in Fig. 1 (see footnote on p. 292). Following a flash, an electron is added to the quinones as long as Q_A is unreduced [10,15]; reaction centers in the state DQ_A^- are photochemically inactive on the time-scale of the reaction with Cyt c^{2+}. The mixture of states present after each flash is determined by the equilibrium partitioning between $Q_A^- Q_B$ and $Q_A Q_B^-$ and between $Q_A^- Q_B^-$ and $Q_A Q_B^{2-}$, described by the partition coefficients α and β, respectively (see Appendix A), where

$$\alpha = \frac{[Q_A^- Q_B]}{[Q_A^- Q_B] + [Q_A Q_B^-]}, \qquad (3)$$

$$\beta = \frac{[Q_A^- Q_B^-]}{[Q_A^- Q_B^-] + [Q_A Q_B^{2-}]}. \qquad (4)$$

The value of β can be obtained by monitoring optically ($\lambda = 550$ nm) the amount of cytochrome oxidized after each of the first three flashes. The absorption change after the first flash (ΔA_1^{550}) corresponds to 1 Cyt c^{2+} oxidized per reaction center, the absorption change after the second flash (ΔA_2^{550}) corresponds to $(1 - \alpha)$ Cyt c^{2+}
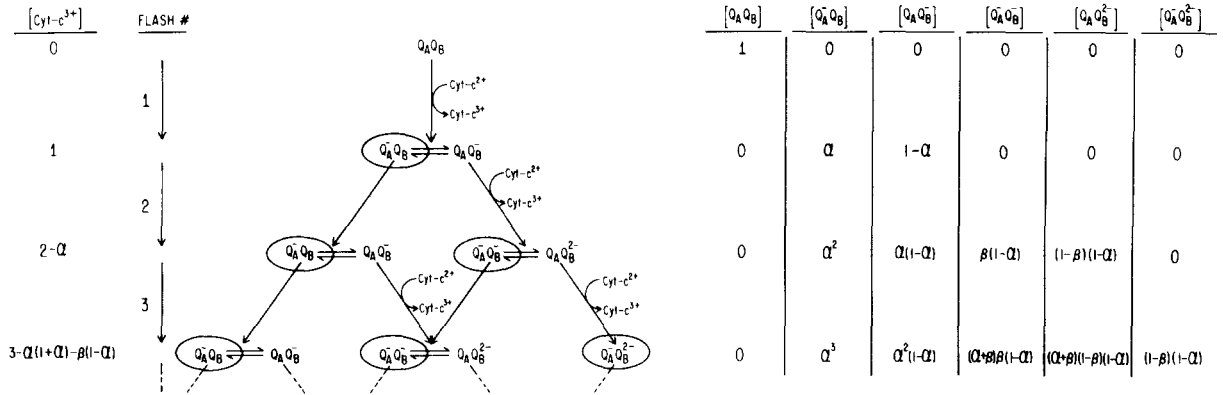
[Cyt-c³⁺]	FLASH #		[Q_AQ_B]	[Q_A⁻Q_B]	[Q_AQ_B⁻]	[Q_A⁻Q_B⁻]	[Q_AQ_B²⁻]	[Q_A⁻Q_B²⁻]
0			1	0	0	0	0	0
1	1		0	α	$1-\alpha$	0	0	0
$2-\alpha$	2		0	α^2	$\alpha(1-\alpha)$	$\beta(1-\alpha)$	$(1-\beta)(1-\alpha)$	0
$3-\alpha(1+\alpha)-\beta(1-\alpha)$	3		0	α^3	$\alpha^2(1-\alpha)$	$(\alpha+\beta)\beta(1-\alpha)$	$(\alpha+\beta)(1-\beta)(1-\alpha)$	$(1-\beta)(1-\alpha)$

Fig. 1. Schematic representation of the various reaction center states after successive flashes in the presence of an exogenous electron donor (e.g., Cyt c^{2+} or DAD). The concentration of the reaction center states and the oxidized exogenous donor, Cyt c^{3+}, are given relative to the initial reaction center concentration. The circled states are those formed immediately after a flash, i.e., at a time short compared to the $Q_A^- Q_B \rightleftharpoons Q_A Q_B^-$ and $Q_A^- Q_B^- \rightleftharpoons Q_A Q_B^{2-}$ equilibration times. It is assumed that the exogenous donor is present in at least a three-fold molar excess and that it reacts with D^+ rapidly compared to the charge recombination of D^+ with either Q_A^- or Q_B^-. The partition coefficients, α and β, are defined by Eqns. 3 and 4 respectively.

oxidized per reaction center, and the absorption change after the third flash (ΔA_3^{550}) corresponds to $(1-\alpha)\{\alpha + (1-\beta)\}$ Cyt c^{2+} oxidized per reaction center (see Appendix B, Eqn. B-2). Thus β is determined from the measured absorption changes using the relation

$$\beta = \frac{\Delta A_1^{550} - \Delta A_2^{550}}{\Delta_1^{550}} + \frac{\Delta A_2^{550} - \Delta A_3^{550}}{\Delta A_2^{550}}, \qquad (5)$$

where the first term corresponds to the partition coefficient α [10]. Eqn. 5 was derived under the assumption that all reaction centers contain exactly two quinones. If the average number of quinones per reaction centers is less than 2.0 but greater than 1.0, one Cyt c^{2+} is still oxidized on the first flash, while on successive flashes the Cyt c^{2+} oxidation depends only on the fraction of reaction centers with two quinones. Eqn. 5 is modified to account for the fraction of reaction centers with one quinone, δ, and becomes

$$\beta = \frac{(1-\delta)\Delta A_1^{550} - \Delta A_2^{550}}{(1-\delta)\Delta A_1^{550}} + \frac{\Delta A_2^{550} - \Delta A_3^{550}}{\Delta A_2^{550}}. \qquad (6)$$

Steady-state semiquinone absorption after successive flashes

An alternative assay to probe the equilibrium partitioning between $Q_A^- Q_B^-$ and $Q_A Q_B^{2-}$ makes use of the optical absorption of the different acceptor states. The ubisemiquinone species Q_A^- and Q_B^- both have a characteristic optical absorption peak at 450 nm [16] that is absent in the neutral quinone and the dihydroquinone (i.e., QH_2) [17]. Thus, the amplitude of the semiquinone absorption after successive flashes can be used to determine the partition coefficients. The relatively strong semiquinone absorption of $Q_A^- Q_B^-$ makes this assay particularly sensitive to the equilibrium between $Q_A^- Q_B^-$ and $Q_A Q_B^{2-}$.

The change in steady-state absorption after the m th flash, ΔA_m^{450}, depends on the concentrations (see Fig. 1) and the extinction coefficients of the semiquinone states. The concentrations, in turn depend only on the partition coefficients α and β (see Appendix A). We confine our analysis to the semiquinone absorption after the first two flashes; these are given by

$$\Delta A_1^{450} = [Q_A^- Q_B]_1 \epsilon_{A^- B}^{450} + [Q_A Q_B^-]_1 \epsilon_{AB^-}^{450} \qquad (7a)$$

$$= [RC]\{\alpha\epsilon_{A^- B}^{450} + (1-\alpha)\epsilon_{AB^-}^{450}\} \qquad (7b)$$

and

$$\Delta A_1^{450} + \Delta A_2^{450} = [Q_A^- Q_B]_2 \epsilon_{A^- B}^{450} + [Q_A Q_B^-]_2 \epsilon_{AB^-}^{450}$$

$$+ [Q_A^- Q_B^-]_2 \epsilon_{A^- B^-}^{450} \qquad (8a)$$

$$= [RC]\{\alpha^2\epsilon^{450}_{A^-B} + \alpha(1-\alpha)\epsilon^{450}_{AB^-}$$

$$+ \beta(1-\alpha)\epsilon^{450}_{A^-B^-}\}, \tag{8b}$$

where [RC] is the concentration of reaction centers and the extinction coefficients $\epsilon^{450}_{A^-B}$, $\epsilon^{450}_{AB^-}$ and $\epsilon^{450}_{A^-B^-}$ refer to the states $Q_A^-Q_B$, $Q_AQ_B^-$ and $Q_A^-Q_B^-$, respectively. The change in absorption after the second flash is (Eqns. 7b and 8b):

$$\Delta A_2^{450} = [RC](1-\alpha)\{\beta\epsilon^{450}_{A^-B^-} - \alpha\epsilon^{450}_{A^-B} - (1-\alpha)\epsilon^{450}_{AB^-}\} \tag{9}$$

Note that the sign of ΔA_2^{450} changes at a critical value of β; for the special case of $\epsilon^{450}_{A^-B} = \epsilon^{450}_{AB^-} = \frac{1}{2}\epsilon^{450}_{A^-B^-}$, this occurs at $\beta = \frac{1}{2}$ (i.e., $[Q_A^-Q_B^-] = [Q_AQ_B^{2-}]$). Combining Eqns. 7b and 9 and solving for β gives

$$\beta = \frac{\epsilon^{450}_{AB^-} + \alpha(\epsilon^{450}_{A^-B} - \epsilon^{450}_{AB^-})}{\epsilon^{450}_{A^-B^-}} \frac{(1-\alpha)\Delta A_1^{450} + \Delta A_2^{450}}{(1-\alpha)\Delta A_1^{450}}. \tag{10}$$

For Eqn. 10 to hold, all reaction centers must contain exactly two quinones. If the average number of less than 2, but greater than 1, $(1-\delta)$ of the reaction centers will remain in the state DQ_A^- after the first flash. Eqn. 10 is modified to account for this contribution and becomes

$$\beta = \frac{\epsilon^{450}_{AB^-} + \alpha(\epsilon^{450}_{A^-B} - \epsilon^{450}_{AB^-})}{\epsilon^{450}_{A^-B^-}} \frac{(1-\alpha)(1-\delta)\Delta A_1^{450} + \Delta A_2^{450}}{(1-\alpha)(1-\delta)\Delta A_1^{450}}.$$

$$\tag{11}$$

The term $(1-\alpha)(1-\delta)\Delta A_1^{450}$ corresponds to the absorption change by the fraction of reaction centers that are photochemically active prior to the second flash.

Electron transfer kinetics between $Q_A^-Q_B^-$ and $Q_AQ_B^{2-}$

In the previous section we discussed the steady-state values of the semiquinone absorption after successive flashes. We now focus on the transient change in semiquinone absorption for reaction centers in the presence of an exogenous electron donor to D^+. We assume that the reaction between the exogenous donor and D^+ is fast compared to the charge recombination between D^+ and the reduced quinone acceptors.

The steady state mixture of states present after a first flash depends on the equilibrium partitioning between $Q_A^-Q_B$ and $Q_AQ_B^-$ (see Fig. 1); $(1-\alpha)$ of the reaction centers are in the photochemically active state $Q_AQ_B^-$. Immediately after the second flash, i.e., at a time $t_0 \ll (k^{obs(1)}_{Q_A^- \to Q_A})^{-1}$, $(k^{obs(2)}_{Q_A^- \to Q_A})^{-1}$, this fraction forms the state $Q_A^-Q_B^-$. Consequently, the change in semiquinone absorption at $t = t_0$ is given by

$$\Delta A_2^{450}(t_0) = [RC](1-\alpha)\{\epsilon^{450}_{A^-B^-} - \epsilon^{450}_{AB^-}\}. \tag{12}$$

The time evolution of the system following the second flash is governed by two parallel processes: (1) reaction centers in the state $Q_A^-Q_B^-$ equilibrate, with rate $k^{obs(2)}_{Q_A^- \to Q_A} = k^{(2)}_{AB} + k^{(2)}_{BA}$, to form a mixture of $Q_A^-Q_B^-$ and $Q_AQ_B^{2-}$. (2) Reaction centers left in the state $Q_A^-Q_B$ reequilibrate, with rate $k^{obs(1)}_{Q_A^- \to Q_A} = k^{(1)}_{AB} + k^{(1)}_{BA}$, to form a mixture of $Q_A^-Q_B$ and $Q_AQ_B^-$. After a time long compared to both of these equilibrium processes the change in absorption reaches the steady-state level $\Delta A_2^{450}(t \to \infty) = \Delta A_2^{450}$ (see Eqn. 9). The transient absorption change, $\Delta A_{trans}^{450}(t)$, leading to this steady-state level is given by

$$\Delta A_{trans}^{450}(t) = \Delta A_2^{450}(t) - \Delta A_2^{450}(t \to \infty) \tag{13a}$$

$$= [RC]\alpha(1-\alpha)(\epsilon^{450}_{A^-B} - \epsilon^{450}_{AB^-})\exp(-k^{obs(1)}_{Q_A^- \to Q_A}t)$$

$$+ [RC](1-\alpha)(1-\beta)\epsilon^{450}_{A^-B^-}\cdot\exp(-k^{obs(2)}_{Q_A^- \to Q_A}t). \tag{13b}$$

The decay kinetics of the transient change (Eqn. 13b) separate into two distinct components when the electron transfer rate between $Q_A^-Q_B$ and $Q_AQ_B^-$ is large compared to that between $Q_A^-Q_B^-$ and $Q_AQ_B^{2-}$, i.e.

$$k^{obs(1)}_{Q_A^- \to Q_A} \gg k^{obs(2)}_{Q_A^- \to Q_A}. \tag{14}$$

Consequently, on the time scale $(k^{obs(1)}_{Q_A^- \to Q_A})^{-1} \ll t \ll (k^{obs(2)}_{Q_A^- \to Q_A})^{-1}$ the decay of the transient absorption change will follow single-exponential kinetics with rate $k^{obs(2)}_{Q_A^- \to Q_A}$. This kinetic behavior is also observed when the relative difference between the extinction coefficients for $Q_A^-Q_B$ and $Q_AQ_B^-$ is small (see Eqn. 13b), i.e.

$$\alpha(\epsilon^{450}_{A^-B} - \epsilon^{450}_{AB^-}) \ll (1-\beta)\epsilon^{450}_{A^-B^-}. \tag{15}$$

The transient change under either or both of the

TABLE I

SEMIQUINONE ABSORPTION $A_{1\,cm}^{450}$ IN REACTION CENTERS FOLLOWING A SINGLE SATURATING FLASH

Reaction centers in 10 mM Tris (pH 8.2)/0.025% (w/v) LDAO/500 μM DAD; $T = 21.5°C$. Typical reaction center concentration was 3.5 μM. o-phen (10 mM) added from a 500 mM solution in EtOH. The reported uncertainties represents the standard deviation of the mean ($n \geqslant 7$). The value of α at pH 8 is 0.065 ± 0.005 [10], $\delta = 0.04 \pm 0.02$ and $\eta = 0.73 \pm 0.02$.

Sample	Quinone Content (Q per RC)	$A_{1\,cm}^{450}/[RC]$ (mM$^{-1}\cdot$cm^{-1})	Expected Contribution
1 Reaction center	1.96 ± 0.02.	6.05 ± 0.06	$(1-\alpha)(1-\delta)\epsilon_{AB}^{450-} +$ $\alpha(1-\delta)\epsilon_{A^-B}^{450} + \delta\epsilon_{A^-}^{450}$
2 Reaction center plus o-phen	1.96 ± 0.02	4.90 ± 0.05	$(1-\delta)\epsilon_{A^-B}^{450} + \delta\epsilon_{A^-}^{450}$
3 Reaction center depleted of Q_B	0.73 ± 0.02	4.36 ± 0.04	$\eta\epsilon_{A^-}^{450}$
4 Reaction Center depleted of Q_B plus o-phen	0.73 ± 0.02	4.21 ± 0.07	$\eta\epsilon_{A^-}^{450}$

above conditions (Eqn. 14 and/or Eqn. 15) is given by

$$\Delta A_{trans}^{450}(t) = [RC](1-\beta)(1-\alpha)\epsilon_{A^-B}^{450} \cdot \exp\left(-k_{Q_A^-\to Q_A}^{obs\,(2)}\,t\right).$$

(16)

If a fraction, δ, of the reaction centers contain only one quinone, Eqn. 16 is modified and becomes

$$\Delta A_{trans}^{450}(t) = [RC](1-\beta)(1-\alpha)(1-\delta)$$
$$\times \epsilon_{A^-B}^{450} \cdot \exp\left(-k_{Q_A^-\to Q_A}^{obs\,(2)}\,t\right).$$

(17)

From Eqn. 17, the extinction coefficient for the state $Q_A^-Q_B^-$ can be determined from the initial amplitude change, $\Delta A_{trans}^{450}(0)$, the measured values of α, β, δ and the concentration of reaction centers.

Experimental results

Extinction coefficients of the semiquinone states

An assay for the partition coefficient β, described in the next section, is based on changes in semiquinone absorption after successive flashes. It was therefore necessary to determine first the extinction coefficients of the semiquinone states $Q_A^-Q_B$, $Q_AQ_B^-$ and $Q_A^-Q_B^-$. The measurements were made at 450 nm, the wavelength at which the

maximum change in semiquinone absorption occurs. The exogenous electron donor was DAD, chosen for its negligible absorption at this wavelength [6].

The steady-state semiquinone absorption after a single saturating flash, $A_{1\,cm}^{450}$, was measured on four different samples (see Table I): (1) reaction centers (2) reaction centers plus 10 mM o-phen (o-phen blocks electron transfer from Q_A^- to Q_B [19,20]), (3) reaction centers that were depleted of

TABLE II

EXTINCTION COEFFICIENTS ϵ^{450} FOR UBISEMIQUINONE ANIONS

The uncertainty is the S.D. of the mean; it does not include the uncertainty in ϵ^{802} ($\pm 5\%$ [13]). Note that the assay for β (see Eqn. 11) depends only on the relative values of the extinction coefficients, not on their absolute value.

Species	Extinction coefficient (mM$^{-1}\cdot$cm^{-1})	Ref.
$Q_AQ_B^-$	$\epsilon_{AB}^{450} = 6.1 \pm 0.1$	this work
$Q_A^-Q_B$	$\epsilon_{A^-B}^{450} = 4.9 \pm 0.1$	this work
$Q_A^-Q_B^-$ [a]	$\epsilon_{A^-B^-}^{450} = 9.7 \pm 0.3$	this work
Q_A^-	$\epsilon_{A^-}^{450} = 5.9 \pm 0.2$	this work
$(UQ-10)^-$ in MeOH	5.4 [b]	22
$(UQ-10)^-$ in DMF	6.0	17

[a] Obtained from a fit of Eqn. 17 to data of Fig. 5d.
[b] A similar value, $\epsilon^{450} = 5$ mM$^{-1}\cdot$cm^{-1}, was reported for $(UQ-10)^-$ in EtOH [17].

Q_B [21], and (4) reaction centers depleted of Q_B plus 10 mM o-phen. For samples (1) and (2), the fraction of reaction centers with a single quinone, δ, was determined (see Materials and Methods) to be 0.04. For samples (3) and (4), the average quinone content, determined by a cytochrome photooxidation assay [14], was $\eta = 0.73$ quinones per reaction center; the low value minimized the fraction of reaction centers with two quinones.

We checked the extent to which o-phen blocked electron transfer by illuminating sample (2) with a second flash after 1 s. If the electron leaks from Q_A^- to Q_B the photochemically active state $Q_A Q_B^-$ is formed. Consequently, an increase in absorption due to the formation of $Q_A^- Q_B^-$ after the second flash should be observed. We found that the increase in absorption was not more than 5%. Thus, on the time scale of the experiments (1 s), o-phen is at least 95% effective in blocking electron transfer.

The measured absorption changes depend on the extinction coefficients $\epsilon_{A^-B}^{450}$, $\epsilon_{AB^-}^{450}$ and $\epsilon_{A^-}^{450}$, as shown in Table I. The measurements on samples (3) and (4) were averaged and, together with the value of η, were used to determine $\epsilon_{A^-}^{450}$. From the absorption of sample (2) and the values of $\epsilon_{A^-}^{450}$ and δ, the extinction coefficient $\epsilon_{A^-B}^{450}$ was determined. The measurements on sample (1), together with the values of $\epsilon_{A^-B}^{450}$, $\epsilon_{A^-}^{450}$, δ and $\alpha = 0.065$ [10], were used to determine $\epsilon_{AB^-}^{450}$.

The individual extinction coefficients are tabulated for pH 8 in Table II. Their value remained, within experimental error, constant between pH 8 and 10. The value of the extinction coefficient for $Q_A^- Q_B^-$, i.e., $\epsilon_{A^-B^-}^{450}$, was determined from the amplitude of the transient absorption change after the second flash (Eqn. 17) (see later section). For comparison, the extinction coefficients of the ubisemiquinone anion measured in organic solvents [17,22] are also tabulated.

The partition coefficient β

Two different assays were used to determine β. In one the concentration of oxidized cytochrome c and in the other the concentration of semiquinone was optically monitored after successive flashes of light.

Cytochrome oxidation after successive flashes. The change in Cyt c^{2+} oxidation after successive

flashes was obtained from the optical absorption changes at 550 nm (see Fig. 2a). There is no absorption by the quinones at this wavelength [16]. The partition coefficient β was computed from the absorption changes after the first three flashes using Eqn. 6. The value of the correction factor, δ, was determined (see Materials and Methods) to be 0.06.

The pH dependence of β is shown in Fig. 2b. The equilibrium between the states $Q_A^- Q_B^-$ and $Q_A Q_B^{2-}$ is strongly pH dependent, with $Q_A Q_B^{2-}$ favored at low pH (i.e., $\beta < 0.5$) and $Q_A^- Q_B^-$ at high pH (i.e., $\beta > 0.5$). The change in the direction
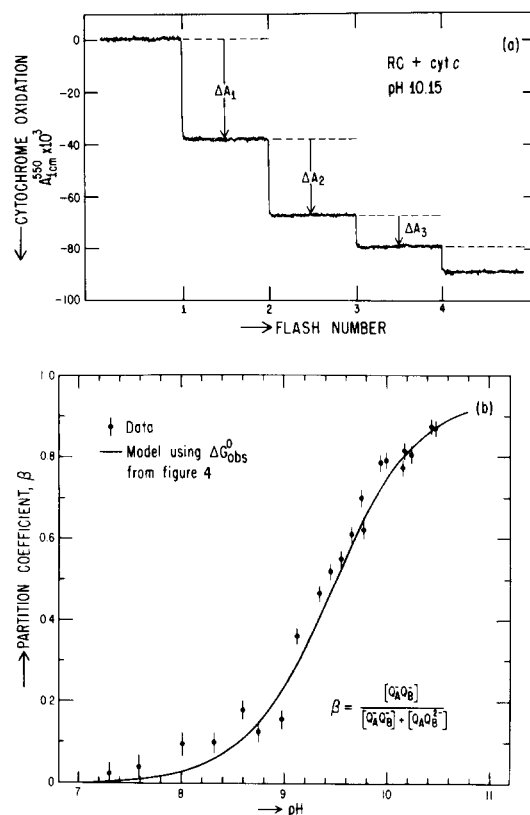

Fig. 2. Determination of the partition coefficient β from the cytochrome oxidation after successive flashes. (a) Changes in the optical absorption measured at pH 10.15. $A_{1\ cm}^{550} = 0$ refers to the absorption level prior to the first flash. Time between flashes 0.6 s. Conditions: 2.1 μM reaction centers and 20 μM Cyt c^{2+} in 10 mM Caps/3.7 mM KCl/0.025% (w/v) LDAO, $T = 21.6°C$. (b) The pH dependence of β. The values were determined (Eqn. 6) from ΔA_1, ΔA_2 and ΔA_3 with $\delta = 0.06$. Conditions same as in part (a), except for varying buffers. Error bars represent the estimated experimental uncertainty (one S.D.). The solid line (Model) was constructed using Eqn. 19 with the free energy shown by the solid line in Fig. 4.

of the equilibrium occurs at approx. pH 9.5. The solid line in Fig. 2b represents a theoretical fit to a model described later.

The method of determining β requires that several conditions, similar to those required fro the determination of α [10], be satisfied. The oxidation of Cyt c^{2+} must be fast compared to the charge recombination of either Q_B^- or Q_B^{2-} with D^+. At low pH this condition is satisfied. However, above pH 9 the Cyt c^{2+} oxidation rate decrease sharply [18], while both charge recombination rates increase with increasing pH (see Ref. 10 and later section). This limited the assay to pH < 10.5. Another requirement is that electrons not leak off from Q_B^- or Q_B^{2-} between flashes. To check this, the time between flashes was varied between 0.3 and 2.0 s; no difference in the value for β was found.

Semiquinone absorption after successive flashes. The steady-state absorption by semiquinone after successive flashes served as the second assay for the partition coefficient β. The experimental results of the absorption changes at two pH values (7.95 and 10.50) are shown in Fig. 3a and b. Note the difference in sign of ΔA_2^{450} between the two sets of data. Qualitatively, the negative value of ΔA_2^{450} in Fig. 3a is a consequence of the diminished semiquinone concentration after the second flash, i.e., the state $Q_A Q_B^{2-}$ is energetically favored. The positive value for ΔA_2^{450} observed at high pH (Fig. 3b) indicates that the equilibrium has shifted in favor of the optically absorbing state $Q_A^- Q_B^-$.

The partition coefficient β was computed from the observed values of ΔA_1^{450}, ΔA_2^{450} and Eqn. 11. The values for the extinction coefficients for the semiquinone states were taken from Table II; δ was determined (see Material and Methods) to be 0.04. The pH dependence of α was determined from the relation (see Eqns. 13 and 14 of Ref. 10)*:

$$\alpha = \frac{1}{1 + \exp\left\{ - \Delta G_{obs\,(1)}^0 / kT \right\}},$$

$$\Delta G_{obs\,(1)}^0 = -67 \text{ meV} - kT \ln\frac{1 + 10^{pH - 11.3}}{1 + 10^{pH - 9.8}}, \tag{18}$$

---

* In principle the partition coefficient α can be determined from ΔA_1^{450} (see Eqn. 7b). However, this method is inaccurate because of the relatively small difference between $\epsilon_{A^-B}^{450}$ and $\epsilon_{AB^-}^{450}$ (see Table II).
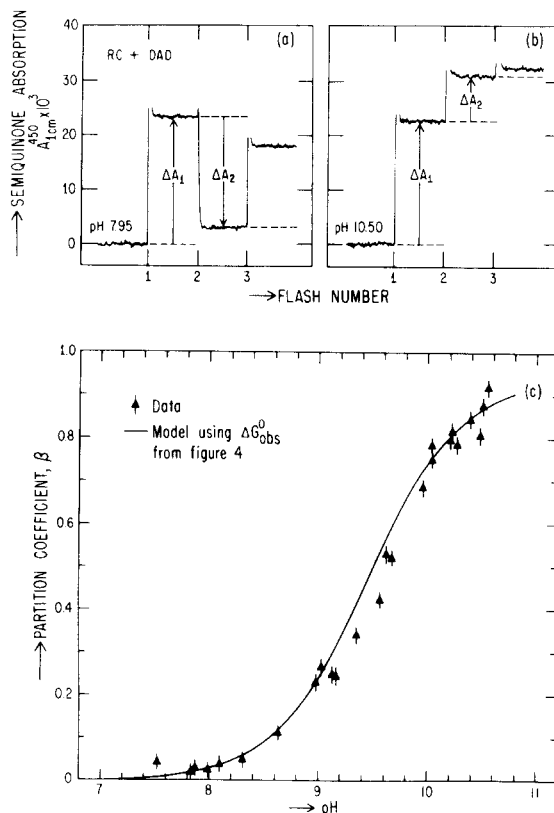

Fig. 3. Determination of the partition coefficient β from the absorption by semiquinone after successive flashes. (a) Changes in the optical absorption measured at pH 7.95. $A_1^{450} = 0$ refers to the absorption level prior to the first flash. Time between flashes 0.6 s. The spikes after each flash are caused by the transient presence of D^+. Conditions: 3.9 μM reaction centers and 500 μM DAD in 10 mM Tris/2.4 mM KCl/0.025% (w/v) LDAO, $T = 21.5°C$. (b) Changes in the optical absorption measured at pH 10.50. Conditions as in part (a), except that 10 mM Caps and 4.4 mM KCl was used. (c) The pH dependence of β. The value of β was determined (Eqn. 11) from ΔA_1 and ΔA_2 with the extinction coefficients shown in Table II, α computed from Eqn. 18 with $\delta = 0.04$. Conditions same as in part (a), except for varying buffering. Error bars represent the estimated experimental uncertainty (one S.D.). The solid line (Model) was constructed using Eqn. 19 with the free energy shown by the solid line in Fig. 4.

where k is Boltzmann's constant and T is the absolute temperature; α varied between 0.07 and 0.28 over the pH range 7–10.6.

The pH dependence of β is shown in Fig. 3c. The results found with this assay are in good agreement with those found by the cytochrome c photooxidation assay (Fig. 2b).

Similarly to the requirement of the cytochrome

c assay, this method requires that the reduction of D^+ by DAD be fast compared to the charge recombination of either Q_B^- or Q_B^{2-} with D^+. The DAD to D^+ electron-transfer rate ($k_{DAD} = 140$ s^{-1}, $[DAD] = 500$ μM, pH 8) is essentially independent of pH [8], while both of the charge recombination rates increase with increasing pH (see Ref. 10 and later section). This limited the assay to a maximum pH of 10.5.

The free-energy difference between $Q_A^- Q_B^-$ and $Q_A Q_B^{2-}$

The free-energy difference, $\Delta G^0_{obs\ (2)}$, between the states $Q_A^- Q_B^-$ and $Q_A Q_B^{2-}$ was obtained from the measured values of the partition coefficient β (see Figs. 2b and 3c), i.e.

$$\Delta G^0_{obs\ (2)} = -kT \ln \frac{[Q_A Q_B^{2-}]}{[Q_A^- Q_B^-]} = -kT \ln \frac{1-\beta}{\beta}. \qquad (19)$$

This relation is useful only when the uncertainty in β is small compared to either β or $(1 - \beta)$. To limit the uncertainty in $\Delta G^0_{obs(2)}$ to less than ± 10 meV, we restricted the analysis to pH > 8.3 for β determined by the cytochrome c assay (Fig. 2b) and to pH > 7.8 for β determined from the semiquinone absorption (Fig. 3c).

Fig. 4 shows the pH dependence of $\Delta G^0_{obs\ (2)}$. Between pH 8 and 10 the free energy increases linearly with pH. In this region the data are well described by the function (see Fig. 4)

$$\Delta G^0_{obs\ (2)} = kT(\ln 10)(pH - pH_0), \qquad (20)$$

where pH_0 is the value (9.5) at which $\Delta G^0_{obs\ (2)} = 0$ (i.e., $\beta = 0.5$); $kT \ln 10 = 58$ meV at 21°C. Above pH 10 the dependence deviates from linearity. The deviation is consistent with a $pK = 10.7$ (see solid line, Fig. 4). The relation of this pK to the protonation of the acceptor complex is discussed in a later section.

The $Q_A^- Q_B^- \rightleftharpoons Q_A Q_B^{2-}$ electron-transfer rate

The electron-transfer rate, $k^{obs\ (2)}_{Q_A^- \to Q_A}$, between $Q_A^- Q_B^-$ and $Q_A Q_B^{2-}$ was determined from the transient absorption change at 450 nm following consecutive flashes in the presence of excess Cyt c^{2+}. To suppress the fast decaying component due to electron transfer between $Q_A^- Q_B$ and $Q_A Q_B^-$ (see
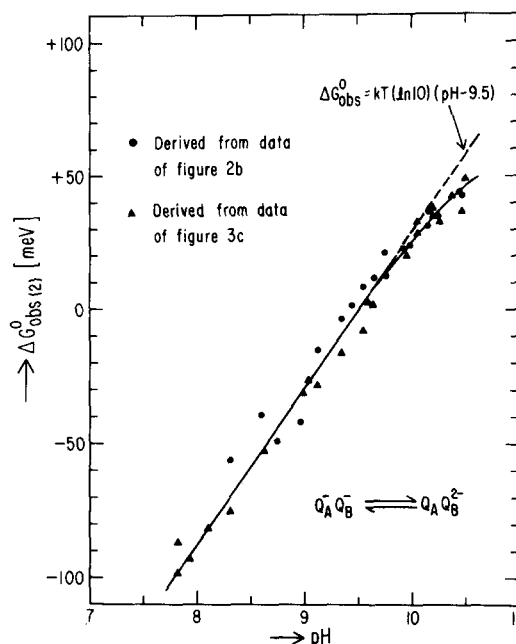

Fig. 4. Free energy difference, $\Delta G^0_{obs(2)}$, between the states $Q_A^- Q_B^-$ and $Q_A Q_B^{2-}$ as a function of pH, $T = 21$°C. The points ($\bullet$, $\blacktriangle$) were obtained from the partition coefficient β (Figs. 2b and 3c and Eqn. 19). The curvature in the solid line through the data corresponds to $pK_B^{(2)} = 10.7$ (see Eqn. 26b).

Eqns. 14 and 16), the instrumental response time was adjusted to attenuate the signal decaying with rate $k^{obs\ (1)}_{Q_A^- \to Q_A}$ (see Fig. 3c in Ref. 10)*. Fig. 5a shows representative data for the absorption changes following the first three flashes. The steady-state absorption following each flash contains contributions from Cyt c^{3+} as well as from the semiquinones. The contribution from Cyt c^{3+}, A^{450}_{Cyt}, was determined from the extinction coefficient $\epsilon^{450}_{ox-red} = 9.0$ $mM^{-1} \cdot cm^{-1}$ [12] and the calculated concentration of Cyt c^{3+} after each flash (Eqn.B-3).

The transfer rate, $k^{obs\ (2)}_{Q_A^- \to Q_A}$, was obtained from the transient absorption change following the second flash, $\Delta A^{450}_{trans}(t)$ (see Fig. 5a). The data were plotted logarithmically, as shown in Fig. 5b, and fitted to straight line. The small transient signal

---

* At pH < 8 the value of $k^{obs\ (2)}_{Q_A^- \to Q_A}$ approaches that of $k^{obs\ (1)}_{Q_A^- \to Q_A}$ (compare Fig. 5c with Fig. 3c in Ref. 10). However, the component decaying with rate $k^{obs\ (1)}_{Q_A^- \to Q_A}$ is at least 100-times smaller than that associated with $k^{obs\ (2)}_{Q_A^- \to Q_A}$. Consequently, the use of the instrumental time constant is not needed to suppress $k^{obs\ (1)}_{Q_A^- \to Q_A}$ (see Eqn. 15).

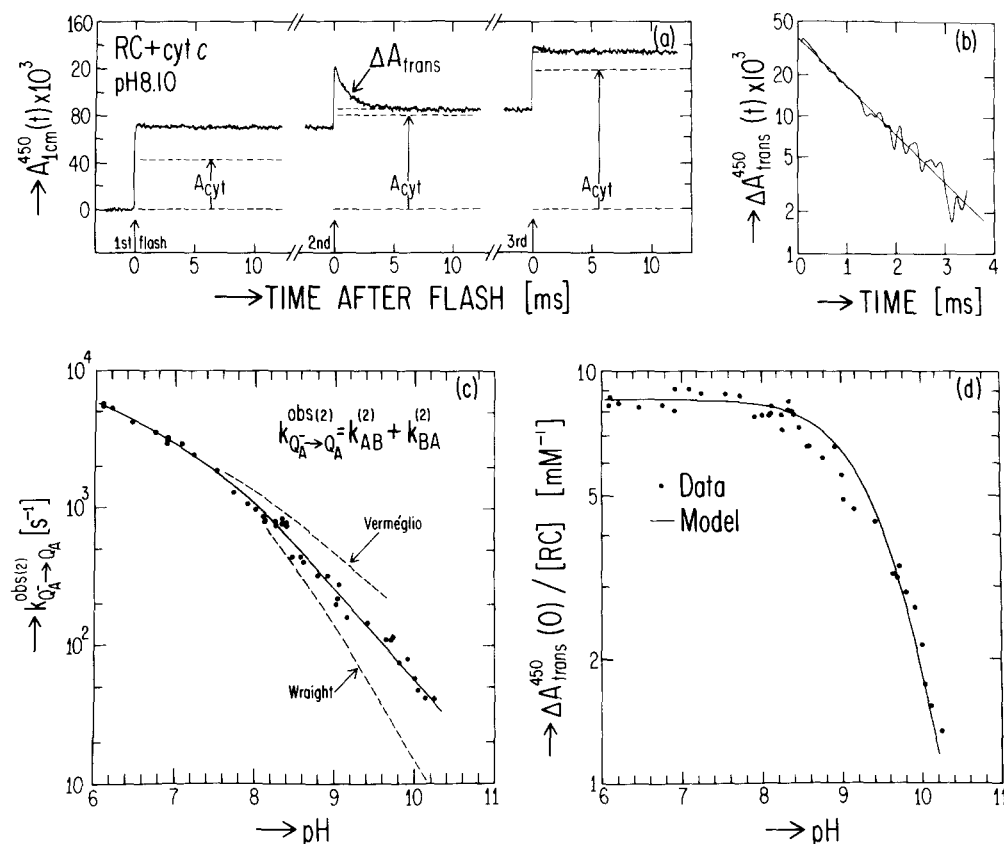Fig. 5. Optical assay for the electron transfer rate, $k^{\mathrm{obs\,(2)}}_{Q_A^- \to Q_A}$, between $Q_A^- Q_B^-$ and $Q_A Q_B^{2-}$. (a) Changes in optical absorption at 450 nm following the first three flashes. $A^{450}_{1\,\mathrm{cm}} = 0$ refers to the absorption level prior to the first flash. Time between flashes, 1.0 s. Conditions: 4.8 μM reaction centers and 50 μM Cyt c^{2+} in 10 mM Tris/3.3 mM KCl/0.025% (w/v) LDAO, pH 8.10 at $T = 21.6^\circ$C. (b) Semilog plot of the transient absorption change, $\Delta A_{\mathrm{trans}}$, following the second flash (see part (a)). The baseline was obtained from the steady-state value of the absorption after the flash. The data were digitally filtered before plotting. The solid line represents a decay rate of $7.9 \cdot 10^2$ s^{-1}. (c) pH dependence of $k^{\mathrm{obs\,(2)}}_{Q_A^- \to Q_A}$. Conditions as in part (a) except for varying buffers. Solid line represents a smooth fit to the data. Dashed lines represent smooth curves drawn through the high pH data reported by Wraight [23] and Vermeglio [24]; at low pH their data follow the solid line. (d) pH dependence of the initial amplitude $\Delta A^{450}_{\mathrm{trans}}(0)$, normalized to the reaction center concentration. The amplitudes were taken from the same data that were used in part (c). The theoretical curve (solid line) was constructed using Eqn. 17 with α calculated from Eqn. 18, β calculated from Eqns. 19 and 20, $\delta = 0.05$ and $\epsilon^{450}_{A^-B^-} = 9.7$ mM$^{-1}\cdot$cm^{-1}.

observed after the third flash results from the fraction of reaction centers that equilibrate between $Q_A^- Q_B^-$ and $Q_A Q_B^{2-}$ (see Fig. 1).

The pH dependence of $k^{\mathrm{obs\,(2)}}_{Q_A^- \to Q_A}$ is shown in Fig. 5c. The rate decreases monotonically with increasing pH; the decrease is less than one decade per pH unit. Results obtained by other workers [23,24] are shown for comparison (see dashed lines in Fig. 5c).

The maximum amplitude of the transient signal, $\Delta A^{450}_{\mathrm{trans}}(0)$, normalized to the concentration of reaction centers, is shown in Fig. 5d. The ampli-

tude of the signal is constant near neutral pH and decreases with increasing pH above approx. pH 8. The decrease occurs as the equilibrium between $Q_A^- Q_B^-$ and $Q_A Q_B^{2-}$ shifts toward $Q_A^- Q_B^-$ at high pH. The decrease in amplitude of the transient signal and the decrease in the Cyt c^{2+} reaction rate with increasing pH [18] limited the measurements to a maximum pH of 10.2.

The solid line through the data of Fig. 5d represents the theoretically predicted amplitude (Eq. 17) using the experimentally determined values for α (Eqn. 18), β (Eqns. 19 and 20), $\delta = 0.05$
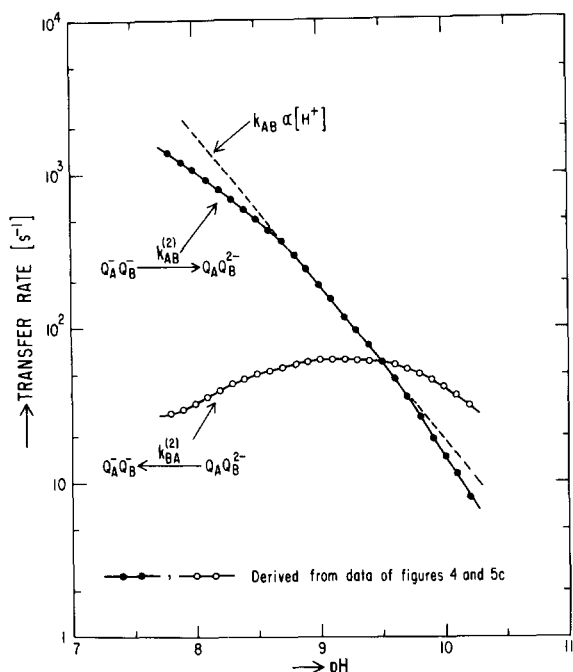
Fig. 6. The forward rate, $k_{AB}^{(2)}$, and the reverse rate, $k_{BA}^{(2)}$, for the $Q_A^- Q_B^-$ to $Q_A Q_B^{2-}$ transition as a function of pH. The points ($\bullet$, $\circ$) were obtained from smooth curves drawn through the data of Figs. 4 and 5c and Eqns. 21 and 22. The dashed curve represents a decrease in $k_{AB}^{(2)}$ of one decade per pH unit (i.e., $k_{AB}^{(2)} \propto [H^+]$).

(see Materials and Methods) and with $\epsilon_{A^-B^-}^{450}$ chosen as a free parameter. The best fit over the entire pH range was found with $\epsilon_{A^-B^-}^{450} = 9.7 \pm 0.3$ mM^{-1} $\cdot$ cm^{-1}.

The electron-transfer rates $k_{AB}^{(2)}$ and $k_{BA}^{(2)}$

The individual forward and reverse transfer rates, $k_{AB}^{(2)}$ and $k_{BA}^{(2)}$, were determined from the observed electron-transfer rate between $Q_A^- Q_B^-$ and $Q_A Q_B^{2-}$ and the free-energy difference between these states using the relations

$$k_{AB}^{(2)} + k_{BA}^{(2)} = k_{Q_A^- \to Q_A}^{obs\,(2)} \qquad (21)$$

and

$$\frac{k_{AB}^{(2)}}{k_{BA}^{(2)}} = \frac{[Q_A Q_B^{2-}]}{[Q_A^- Q_B^-]} = \exp \frac{-\Delta G_{obs\,(2)}^0}{kT}. \qquad (22)$$

From smooth curves drawn through the data in Figs. 4 and 5c (see solid lines), the pH dependence of $k_{AB}^{(2)}$ and $k_{BA}^{(2)}$ was obtained, as shown in Fig. 6.

The forward transfer rate $k_{AB}^{(2)}$ decreases with increasing pH at the rate of approximately one decade per pH unit (i.e., $k_{AB}^{(2)} \propto [H^+]$) over the major part of the pH range investigated (see dashed line). The reverse rate $k_{BA}^{(2)}$ is only weakly dependent on pH, varying approx. 75-times less than $k_{AB}^{(2)}$ over the same pH range.

Preparation of $DQ_A Q_B^-$ in the absence of exogenous donors

The charge recombination kinetics of $D^+ Q_A Q_B^{2-}$ must be studied in the absence of an exogenous donor to D^+. However to prepare the precursor state, $DQ_A Q_B^-$, a donor, such as Cyt c^{2+}, is required. The fulfillment of these seemingly contradictory conditions requires an initial molar ratio of Cyt c^{2+} to reactions centers of one. Since the extinction coefficients ϵ_{red}^{550} of Cyt c^{2+} and ϵ^{802} of reaction centers are not known with sufficient accuracy, we determined spectroscopically the condition for equal molarity and in the process obtained an accurate value for the ratio $\epsilon^{802}/\epsilon_{red}^{550}$.

The assay is based on monitoring the extent of cytochrome oxidation after the second flash. When the initial Cyt c^{2+} concentration, $[Cyt\ c^{2+}]_0$, is less than the reaction center concentration, all of the Cyt c^{2+} is oxidized after the first flash. Consequently, no change in cytochrome absorption is expected after the second flash. When the initial cytochrome concentration is between 1- and 2- (precisely, $1 + (1 - \alpha)(1 - \delta)$)-times the reaction center concentration, the absorption change after the first flash ΔA_1^{550} is proportional to $[Cyt\ c^{2+}]_0$; the absorption change after the second flash ΔA_2^{550} is proportional to the remaining Cyt c^{2+}, i.e., $[RC] - [Cyt\ c^{2+}]_0$. Relating the initial concentrations of cytochrome and reaction centers to their respectively absorption maxima at 550 nm and 802 nm gives

$$\frac{\Delta A_2^{550}}{\Delta A_1^{550}} = \begin{cases} 0 & ;\text{if } 0 < [Cyt\ c^{2+}]_0 \leqslant [RC] \\ \dfrac{\epsilon^{802}}{\epsilon_{red}^{550}} \dfrac{A_{Cyt}^{550}}{A_{RC}^{802}} - 1 & ;\text{if } [RC] < [Cyt\ c^{2+}]_0 \leqslant [RC] \\ & \qquad \times \{1 + (1 - \alpha)(1 - \delta)\} \end{cases} \qquad (23)$$

The condition for equal initial concentrations is found by fitting Eqn. 23 to the measured absorp-

tion changes with $\epsilon^{802}/\epsilon_{red}^{550}$ taken as a free parameter.

Fig. 7 shows the extent of the flash-induced oxidation of Cyt c^{2+} as a function of the ratio $A_{Cyt}^{550}/A_{RC}^{802}$. The absorption A_{Cyt}^{550} was determined prior to the addition of reaction centers. The absorption A_{RC}^{802} was measured after the photooxidation measurements. The onset of light-induced oxidation of Cyt c^{2+} after the second flash corresponds to the condition $[\text{Cyt } c^{2+}]_0 = [\text{RC}]$. From a fit of Eqn. 23 to the data (Fig. 7) this occurs for $A_{Cyt}^{550}/A_{RC}^{802} = 0.094 \pm 0.003$ (S.D. of the mean), corresponding to a ratio of extinction coefficients

$$\frac{\epsilon^{802}}{\epsilon_{red}^{550}} = 10.6 \pm 0.3, \tag{24}$$

The result given by Eqn. 24 is consistent with $\epsilon^{802}/\epsilon_{red}^{550} = 9.2$–10.9 computed from the range of values reported for the extinction coefficients of reaction centers [13,25] and cytochrome c^{2+} (see tabulations in Refs. 26 and 27).

In the above analysis we assumed that the reaction between Cyt c^{2+} and D^+ goes to impletion. In practice, the finite redox free-energy difference between the two species prevents the complete reduction of D^+; for the condition $[\text{Cyt } c^{2+}]_0 = [\text{RC}]$, approx. 3% of the reaction centers will have their donor, D^+, unreduced by Cyt c^{2+} after a flash (see Appendix D).

The donor recovery rate $k_{D^+ \to D}^{obs\ (2)}$

The donor recovery kinetics for reaction centers in the presence of an equal molar ratio of Cyt c^{2+} was monitored at 865 nm. The results at pH 8.1 are shown in Fig. 8a. The absorption change after the first flash corresponds to the formation of $DQ_AQ_B^-$. The oxidation of D^+ by Cyt c^{2+} is fast compared to the instrumental time constant; consequently, the observed amplitude is small. The absorption change following the second flash corresponds to the formation and subsequent decay of $D^+Q_AQ_B^{2-}$; a fast component due to the oxidation of Cyt c^{2+} remaining after the first flash is not resolved. The changes following the third and fourth flash were, within experimental resolution, identical to each other; this indicates that $DQ_AQ_B^-$ is stable on the time-scale of the measurements. The amplitude of the absorption change after the

second flash was approx. 6% smaller than that after the third flash. Approx. 3% of this difference is due to the finite redox free-energy difference between Cyt c^{2+} and D^+ (see Appendix D); the remainder (2–3%) may be caused by a fraction of reaction centers having an impaired Cyt c binding site.

The charge recombination rate was determined from the slope of the logarithm of the absorption change following the second flash (see Fig. 8b). The decay kinetics consist primarily of a slow component (approx. 80%) with rate $k_{D^+ \to D}^{obs\ (2)} = 0.75$ s^{-1} (dashed line in Fig. 8a); the remaining (approx. 20%) component decays approx. 5-times faster ($k^{obs} = 3.5\ s^{-1}$).

The predicted rate for charge recombination via the intermediate state $D^+Q_A^-Q_B^-$ is $k_{D^+ \to D}^{obs\ (2)} = \beta k_{AD}^{(2)}$ (see Eqn. 2b). The average value for β at pH 8.1, found from the data of Figs. 2b and 3c, is 0.07 ± 0.02. The recombination rate of $D^+Q_A^-$ is $k_{AD}^{(1)} = 10\ s^{-1}$, independent of pH [10]. Making the assumption that $k_{AD}^{(2)} = k_{AD}^{(1)}$, the recombination rate predicted for the indirect pathway $\beta k_{AD}^{(1)} = 0.7$ $\pm 0.2\ s^{-1}$. This value is in agreement with the rate observed for the slow component (0.75 s^{-1}) of the charge recombination (Fig. 8b). Thus, the contribution to the slow component from direct recombination between Q_B^{2-} and D^+, obtained from the maximum discrepancy between the observed recovery rate and the rate predicted for the indirect
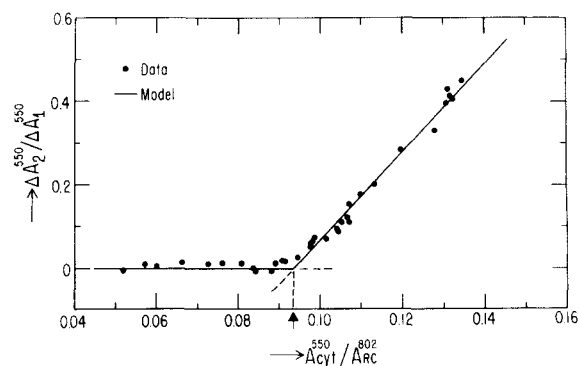

Fig. 7. Optical assay of the relative extinction coefficients of reaction center and cytochrome c^{2+}. The absorption changes ΔA_1^{550} and ΔA_2^{550} were measured as shown in Fig. 2a. Conditions: 2.1–5.2 μM reaction centers and 3.7 μM Cyt c^{2+} in 10 mM Tris/3.3 mM KCl/0.025% (w/v) LDAO, pH 8.0 at $T = 21.5°C$. The theoretical curve (solid line) was constructed using Eqn. 23 with $(\epsilon^{802}/\epsilon_{red}^{550}) = 10.6$.

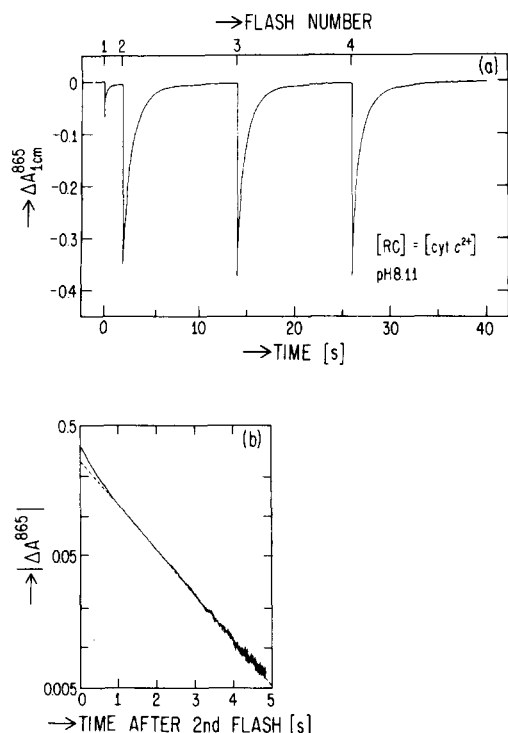Fig. 8. (a) Optical assay for the donor recovery rate, $k^{obs\,(2)}_{D^+\to D}$. Time interval between the first and second flash 2 s; between the second and successive flashes 13 s. Conditions: 3.7 μM reaction centers and 3.7 μM Cyt c^{2+} (precisely, [Cyt $c^{2+}]_0/[RC] = 1.00 \pm 0.03$) in 10 mM Tris/3.3 mM KCl/0.025% (w/v) LDAO, pH 8.09 at $T = 21.2°C$. (b) Semi-logarithmic plot of the absorption change after the second flash (see part (a)). The dashed line corresponds to a recovery rate of 0.75 s^{-1}. The same value was obtained after the third and forth flashes.

pathway, accounts for less than 30% of the decay rate.

Above pH 8, the decay rate of the slow component of the recovery kinetics increased and was in agreement with the values predicted for the indirect pathway. However, the fractional contribution of the slow component to the kinetics decreased with increasing pH; the amplitude of the faster decaying component being dominant above pH $\approx$ 8.5. The decay rate of the faster component reached a value 12 s^{-1} at pH 10. Above pH 10 the reaction rate of Cyt c^{2+} with D$^+$ is too slow to effectively generate DQ$_A$Q$_B^-$.

Below pH 8 the recovery kinetics following the second flash became non-exponential in character; i.e., the decay rate constant increased with increas-
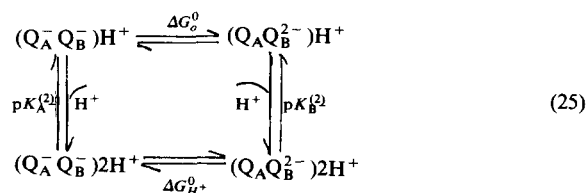
ing time. This behavior was independent of the time interval (2–20 s) between the first and second flash. Furthermore, the recovery kinetics following the third flash was substantially faster than the kinetics following the second flash. Because of these difficulties, the charge recombination kinetics of D$^+$Q$_A$Q$_B^{2-}$ could not be properly assessed at low pH.

Conclusion and Discussion

The pH dependence of $\Delta G^0_{obs\,(2)}$

We have investigated electron equilibria and transfer reactions involving the quinone acceptor complex in bacterial reaction centers. From the equilibrium data we deduced the free energy difference between Q$_A^-$Q$_B^-$ and Q$_A$Q$_B^{2-}$. We found that the free energy difference increases with increasing pH (7.8 < pH < 10.5). The state Q$_A$Q$_B^{2-}$ is energetically favored near neutral pH, whereas Q$_A^-$Q$_B^-$ is favored at high, nonphysiological, pH. It is the preferential interaction of a proton with Q$_A$Q$_B^{2-}$ that provides the driving force for the electron transfer to occur in the forward direction.

To examine quantitatively the role of protonation on the stabilization of Q$_B^{2-}$, the equilibrium between Q$_A^-$Q$_B^-$ and Q$_A$Q$_B^{2-}$ was modeled by the scheme shown in Eqn. 25. For the pH range used in this study, the one-electron precursor state Q$_A$Q$_B^-$ associates with a proton (p$K_B^{(1)} = 11.3$) [10]. The two-electron states are in equilibrium with a second proton as shown:

$$(Q_A^- Q_B^-)H^+ \overset{\Delta G^0_o}{\rightleftharpoons} (Q_A Q_B^{2-})H^+$$

$$pK_A^{(2)} \Big\updownarrow H^+ \qquad H^+ \Big\updownarrow pK_B^{(2)} \qquad (25)$$

$$(Q_A^- Q_B^-)2H^+ \underset{\Delta G^0_{H^+}}{\rightleftharpoons} (Q_A Q_B^{2-})2H^+$$

The measured free energy, $\Delta G^0_{obs\,(2)}$, involves both the protonated and unprotonated species and is given by [10]

$$\Delta G^0_{obs\,(2)} = -kT \ln \frac{[(Q_A Q_B^{2-})H^+] + [(Q_A Q_B^{2-})2H^+]}{[(Q_A^- Q_B^-)H^+] + [(Q_A^- Q_B^-)2H^+]} \quad (26a)$$

$$= \Delta G^0_{H^+} - kT \ln \frac{1 + 10^{pH - pK_B^{(2)}}}{1 + 10^{pH - pK_A^{(2)}}}. \quad (26b)$$

For the pH range $pK_A^{(2)} \ll pH \ll pK_B^{(2)}$, Eqn. 26b reduces to (cf. Eqn. 20):

$$\Delta G^0_{obs(2)} = \Delta G^0_{H^+} + kT(\ln 10)\left(pH - pK_A^{(2)}\right) \qquad (27)$$

From the pH dependence of $\Delta G^0_{obs(2)}$ (See Fig. 4) the pK values for the association of a second proton with either $Q_A^- Q_B^-$ or $Q_A Q_B^{2-}$ can be obtained. The linear pH dependence of $\Delta G^0_{obs(2)}$ at low pH places a limit on the pK for the equilibrium between $(Q_A^- Q_B^-)H^+$ and $(Q_A^- Q_B^-)2H^+$, i.e. (see Eqns. 26b and 27):

$$pK_A^{(2)} < 8 \qquad (28)$$

The pK for the equilibrium between $(Q_A Q_B^{2-})H^+$ and $(Q_A Q_B^{2-})2H^+$ was obtained from the curvature in $\Delta G^0_{obs(2)}$ (Fig. 4) at high pH. However, in view of the difficulty in measuring β at high pH, we establish only the tentative value (see Eqn. 26b):

$$pK_B^{(2)} \geqslant 10.7 \qquad (29)$$

These results imply that electron transfer from $Q_A^- Q_B^-$ to $Q_A Q_B^{2-}$ involves the stabilization of Q_B^{2-} by the association of a second proton with the acceptor complex. The stabilization energy of $Q_A Q_B^{2-}$ relative to $Q_A^- Q_B^-$ is $kT(\ln 10)(pK_B^{(2)} - pK_A^{(2)}) > 160$ meV.

The pK for the protonation of Q_A^- in the presence of Q_B^-, i.e., $pK_A^{(2)}$, is considerably lower than that for the protonation of $Q_A^- Q_B$ ($pK_A^{(1)} = 9.8$) [10,28-30]. This implies that the charge on Q_B^- decreases the interaction energy of Q_A^- with a proton by $kT(\ln 10)(pK_A^{(1)} - pK_A^{(2)}) > 100$ meV.

The value of $\Delta G^0_{obs(2)}$ found in this study is similar to the one obtained for Photosystem II in chloroplasts [31-34]. Diner [33] found $\Delta G^0_{obs(2)} \approx -100$ meV in dark adapted chloroplasts (pH 7.5), which is close to the value found for the bacterial system at pH 8 (see Fig. 4)*. The equilibrium in illuminated chloroplasts was found to shift away from $Q_A Q_B^{2-}$ [33]. This effect may be related to the pH dependence of $\Delta G^0_{obs(2)}$. Under illumina-

tion the pH on the acceptor side of the chloroplast membranes rises (see, e.g., Ref. 1), thereby increasing $\Delta G^0_{obs(2)}$ (see Fig. 4). Thus, the increase in $\Delta G^0_{obs(2)}$ with increasing pH seems to serve as a feedback mechanism to limit the rise in intracellular pH.

The relation of $\Delta G^0_{obs(2)}$ to redox titrations and proton uptake

The free energy difference between the states $Q_A^- Q_B^-$ and $Q_A Q_B^{2-}$ is equal to the difference in reduction-oxidation (redox) energies between the $Q_A Q_B^- / Q_A^- Q_B^-$ and the $Q_A Q_B^- / Q_A Q_B^{2-}$ couples. The pH dependence of the redox couples that yield the free energy difference found between the states $Q^- Q_B^-$ and $Q_A Q_B^{2-}$ (see solid line in Fig. 4) is shown in Fig. 9. These curves were computed using the relation [10,35]

$$G^{redox}_{Q_A Q_B^- / Q_A Q_B^-} = G^0_{(Q_A Q_B^-)2H^+} - kT \ln \frac{1 + 10^{pH - pK_A^{(2)}}}{1 + 10^{pH - pK_0}}, \qquad (30)$$

with an equivalent expression for $G^{redox}_{Q_A Q_B^- / Q_A Q_B^{2-}}$. Note that pK_0 describes the protonation of the neutral species Q_A; it is less than $pK_A^{(2)} < 8$ and therefore does not enter into the analysis.

The reduction of Q_A in the presence of Q_B^- is not associated with a protonation step and thus the redox energy for the couple $Q_A Q_B^- / Q_A^- Q_B^-$ is pH independent (see Fig. 9). The second reduction of Q_B^-, to form Q_B^{2-}, is associated with the uptake of a proton and thus the redox energy for the couple $Q_A Q_B^- / Q_A Q_B^{2-}$ is proportional to pH (approx. 60 meV per pH unit). By combining the results for the pH dependence of the one-electron [10] and two-electron redox couples, the overall sequence for the protonation steps accompanying the successive reduction of the quinone acceptor complex is obtained, as shown in Fig. 10. Models for the uptake of protons by the acceptor complex have been proposed by Wraight [23].

The scheme shown in Fig. 10 predicts that the formation of Q_B^{2-} is accompanied by the uptake of two protons per reaction center. The overall stoichiometry of two protons per Q_B^{2-} is in agreement with experimental observation [23,36,37]. However, the stoichiometry of protonation following transfer of the first electron to Q_B is controversial [23,36-39].

---

* The value $\Delta G^0_{obs(1)} \approx -75$ meV (pH 7.5) found in chloroplasts [29,33,50] is also close to the value found for bacterial systems [10,11,51].

The electronic currents and/or voltage associated with the transfer steps between Q_A and Q_B have been studied with reaction centers in lipid layers [40–43]. No current was found to accompany the electron transfer between $Q_A^- Q_B$ and $Q_A Q_B^-$. However, an electric signal was observed to accompany the electron transfer from $Q_A^- Q_B^-$ to $Q_A Q_B^{2-}$ (Ref 43; see also Blatt, Y., Gopher, A., Kleinfeld, D., Montal, M. and Feher, G. unpublished results). The difference in behavior between the two cases may be related to the different protonation steps associated with the transfer of the first and second electron. In the $Q_A^- Q_B$ to $Q_A Q_B^-$ transition both states associate with a proton (see Fig. 10), suggesting that the electronic current is counterbalanced by a concomitant pro-
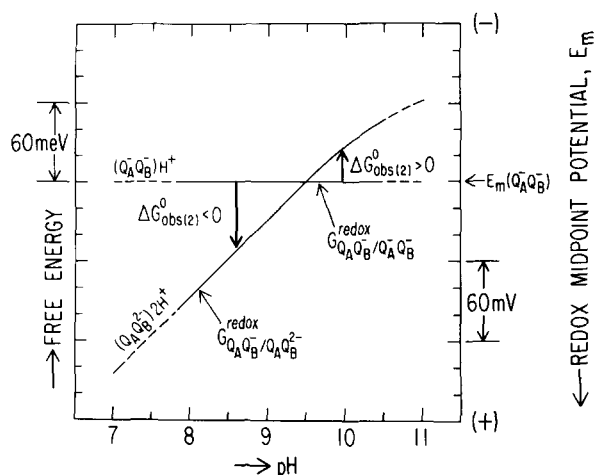

Fig. 9. The pH dependence of the redox free energy, or equivalently, the redox midpoint potential, of the $Q_A Q_B^-/Q_A^- Q_B^-$ and $Q_A Q_B^-/Q_A Q_B^{2-}$ couples (compare with the pH dependence of the one-electron couples shown in Fig. 8 of Ref. 10). The curves were constructed using the expression for $G_{Q_A Q_B^-/Q_A Q_B^-}^{redox}$ (Eqn. 30) with $pK_A^{(2)} \ll 8$ and $T = 21.5°C$ and the equivalent expression for $G_{Q_A Q_B^-/Q_A Q_B^{2-}}^{redox}$ with $pK_B^{(2)} = 10.7$. The difference between the two curves was established from the values of $\Delta G_{obs\ (2)}^0$, and represents the energy difference between the states $Q_A^- Q_B^-$ and $Q_A Q_B^{2-}$, as shown in Fig. 4. The dashed part of the curves is an extrapolation beyond the range for which energy differences were experimentally determined. Note the change in sign of $\Delta G_{obs\ (2)}^0$ (i.e., reversal of equilibrium) at the crossing point of the two curves. The midpoint potential of the $Q_A Q_B^-/Q_A Q_B^{2-}$ couple, measured in chromatophores [29], is $E_m(Q_A Q_B^{2-}) = -40$ meV at pH 8. This suggests that the midpoint potential of the $Q_A Q_B^-/Q_A^- Q_B^-$ couple (with Q_A^- unprotoned and Q_B^- protonated) is $E_m(Q_A^- Q_B^-) = -130$ meV, close to the potential for the unprotonated form of the $Q_A Q_B/Q_A^- Q_B$ couple [28–30].

ton current. In contrast, Q_A^- does not associate with a proton in the $Q_A^- Q_B^-$-to-$Q_A Q_B^{2-}$ transition (see Fig. 10).

The pH dependence of the electron transfer rates between $Q_A^- Q_B^-$ and $Q_A Q_B^{2-}$

The electron-transfer rate from $Q_A^- Q_B^-$ to $Q_A Q_B^{2-}$ was first determined at pH 7.5 by Verméglio and Clayton [16]. The pH dependence of this rate was subsequently measured by Wraight [23] and Verméglio [24]. Both investigators found $k_{Q_A^- \to Q_A}^{obs\ (2)}$ to decrease with increasing pH; below approx. pH 8 the decrease is similar to that reported here (see Fig. 5c). At high pH, the values for $k_{Q_A^- \to Q_A}^{obs\ (2)}$ found in this study fall between those reported by Wraight [23] and Verméglio [24] (see dashed lines in Fig. 5c).

The pH dependence of the observed transfer rate is dominated by the forward rate $k_{AB}^{(2)}$ (Fig. 6). This results from the stabilization of $Q_A Q_B^{2-}$ relative to $Q_A^- Q_B^-$ through the association of Q_B^{2-} with a proton. If the forward electron transfer is limited by the rate at which a proton binds to the reaction center, as suggested by Wraight [23], $k_{AB}^{(2)}$ should be proportional to $[H^+]$. The reverse rate $k_{BA}^{(2)}$ should be independent of pH, since the electron transfer to regenerate $Q_A^- Q_B^-$ involves the release of a proton. This is in approximate agreement with the results shown in Fig. 6.

The charge recombination kinetics $D^+ Q_A Q_B^{2-} \to D Q_A Q_B^-$

When the acceptor states $Q_A^- Q_B^-$ and $Q_A Q_B^{2-}$ are in equilibrium on a time-scale of the charge recombination of $D^- Q_A Q_B^{2-}$, the donor recovery is expected to follow single-exponential kinetics. This condition holds irrespective of whether the electron originates from $Q_A^- Q_B^-$, $Q_A Q_B^{2-}$ or both (see Appendix in Ref. 10). The observation of recombination kinetics that deviate from an exponential time dependence implies either a distribution of reaction centers having different recombination rates or the presence of an additional state (or states) in the charge recombination pathway. The new state must equilibrate with the other reaction center states (see Eqn. 2a) at a rate not greater than $k_{D^+ \to D}^{obs\ (2)}$.

Between pH 8 and 9 the observed kinetics of recombination could be decomposed into two exponentials, differing in rate constants by a factor

of approx 5. The slower rate agreed with the predicted charge recombination via the intermediate state $D^+ Q_A^- Q_B^-$ under the assumption that $k_{AD}^{(2)} = k_{AD}^{(1)}$. This assumption seems justified in view of the insensitivity of $k_{AD}^{(1)}$ to changes in the free energy of Q_A^- [44,45], such as may be caused by the charge on Q_B^-. The origin of the faster decay process is at present not understood. One possibility is that reaction centers exist in a pH dependent mixture of two (or more) conformational states having different values of $k_{BD}^{(2)}$. In one of the conformational states direct recombination between Q_B^{2-} and D^+ is the dominant (fast) process.

Below pH 8 the donor recovery kinetics exhibited a complicated time dependence. Furthermore, the recovery kinetics following the second and third flashes differed substantially from each other. In analogy with the explanation for the kinetics at high pH, the behavior at low pH may reflect a transition between conformational states. One of the states may be stabilized only after the formation of $D^+ Q_A Q_B^{2-}$ (i.e., after the second flash). The binding of Q_B^{2-} to reaction centers is reported to be weaker than the binding of either Q_B or Q_B^- [46]. Thus a possible transition may involve the rearrangement of Q_B^{2-} in the binding site of the secondary quinone.

Concluding remarks

In this and our preceding work [10], we described how protons are involved in the electron transfer between the primary and secondary acceptor in bacterial reaction centers. Our description was based on measurements of the thermodynamic and kinetic relations for the $Q_A^- Q_B \rightleftharpoons Q_A Q_B^-$ and $Q_A^- Q_B^- \rightleftharpoons Q_A Q_B^{2-}$ equilibria. We showed previously [10] that the uptake of a proton provides the driving force for the transfer of the first electron to Q_B. The same was found in the present work to hold for the second electron, whose transfer to Q_B^- is accompanied by the uptake of a second proton. The uptake of protons that accompanies the sequential reduction of the quinone acceptor complex is the starting point for the transduction of light into a proton gradient across the cell membrane. The final state Q_B^{2-} transfers electrons and protons to exogenous (quinone) acceptors. This process, the details of which re-
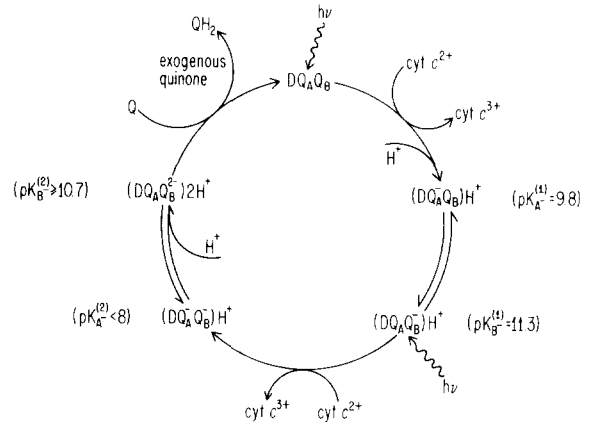

Fig. 10. Schematic representation of the protonation events in reaction centers following successive flashes of light in the presence of Cyt c^{2+} and exogenous quinone. The scheme is based on the free energy and kinetic relations between the states $Q_A^- Q_B$ and $Q_A Q_B^-$ presented previously [10], and the relations between the states $Q_A^- Q_B^-$ and $Q_A Q_B^{2-}$ found in this study. The pK values for each protonation step are shown in parenthesis; the scheme was drawn for $pK_A^{(2)} < pH < pK_A^{(1)}$.

main to be worked out, provides a pathway for the return of electrons to the primary donor concomitant with the undirectional transport of protons across the membrane.

Acknowledgements

Appendix A. Reaction center states after successive flashes

The concentration of the different reaction center states after m successive flashes (see Fig. 1) are described by the difference equations:

$$[Q_A^- Q_B]_m = \alpha([Q_A Q_B]_{m-1} + [Q_A^- Q_B]_{m-1}), \qquad (A\text{-}1a)$$

$$[Q_Q Q_B^-]_m = (1-\alpha)([Q_A Q_B]_{m-1} + [Q_A^- Q_B]_{m-1}), \quad (A\text{-}1b)$$

$$[Q_A^- Q_B^-]_m = \beta([Q_A Q_B^-]_{m-1} + [Q_A^- Q_B^-]_{m-1}), \qquad (A\text{-}1c)$$

$$[Q_A Q_B^{2-}]_m = (1-\beta)([Q_A Q_B^-]_{m-1} + [Q_A^- Q_B^-]_{m-1}), (A\text{-}1d)$$

$$[Q_A^- Q_B^{2-}]_m = [Q_A Q_B^{2-}]_{m-1} + [Q_A Q_B^{2-}]_{m-1}. \qquad (A\text{-}1e)$$

where α and β are defined by Eqns. 3 and 4. The reaction center states satisfy the conservation equation

$$[Q_A Q_B]_m + [Q_A^- Q_B]_m + [Q_A Q_B^-]_m + [Q_A^- Q_B^-]_m$$
$$+ [Q_A Q_B^{2-}]_m + [Q_A^- Q_B^{2-}]_m = [RC], \qquad (A-2)$$

where $[RC]$ is the concentration of reaction center. The initial conditions are given by

$$[Q_A Q_B]_0 = [RC], \qquad (A-3a)$$

$$[Q_A^- Q_B]_0 = [Q_A Q_B^-]_0 = [Q_A^- Q_B^-]_0 = [Q_A Q_B^{2-}]_0$$
$$= [Q_A^- Q_B^{2-}]_0 = 0. \qquad (A-3b)$$

The solution of the difference equations, for $m > 1$, are given by:

$$[Q_A Q_B]_m = 0, \qquad (A-4a)$$

$$[Q_A^- Q_B]_m = [RC]\alpha^m, \qquad (A-4b)$$

$$[Q_A Q_B^-]_m = [RC](1-\alpha)\alpha^{m-1}, \qquad (A-4c)$$

$$[Q_A^- Q_B^-]_m = [RC]\beta(1-\alpha)\frac{\alpha^{m-1}-\beta^{m-1}}{\alpha-\beta}, \qquad (A-4d)$$

$$[Q_A Q_B^{2-}]_m = [RC](1-\beta)(1-\alpha)\frac{\alpha^{m-1}-\beta^{m-1}}{\alpha-\beta}, \qquad (A-4e)$$

$$[Q_A^- Q_B^{2-}]_m = [RC]\left\{1 - \frac{(1-\beta)\alpha^{m-1}-(1-\alpha)\beta^{m-1}}{\alpha-\beta}\right\}. \qquad (A-4f)$$

Note that for the special case $\alpha = \beta$,

$$\lim_{\alpha \to \beta} \frac{\alpha^m - \beta^m}{\alpha - \beta} = m\alpha^{m-1}$$

After many flashes (i.e., as $m \to \infty$), the concentration of all states, except $Q_A^- Q_B^{2-}$, tend toward zero; the concentration of $Q_A^- Q_B^{2-}$ tends toward $[RC]$.

Appendix B. Cytochrome oxidation after successive flashes

The change in absorption caused by the oxidation of Cyt c^{2+} by D^+ after successive flashes is most conveniently measured at $\lambda = 550$ nm (see Fig. 2a). The change in absorption after the mth flash is given by

$$\Delta A_m^{550} = -\epsilon_{red-ox}^{550}\Delta[\text{Cyt } c^{3+}]_m \qquad (B-1a)$$

$$= -\epsilon_{red-ox}^{550}\left\{[Q_A Q_B]_{m-1} + [Q_A Q_B^-]_{m-1}\right.$$
$$\left. + [Q_A Q_B^{2-}]_{m-1}\right\} \qquad (B-1b)$$

where the expression in the brackets represents the concentration of photochemically active reaction centers present before the flash (see Fig. 1). Substituting Eqns. A-4a, A-4c and A-4f, the change in absorption can be expressed in terms of α and β, i.e.,

$$\Delta A_m^{550} = -[RC]\epsilon_{red-ox}^{550}\begin{cases} 1 & \text{if } m=1; \\ \dfrac{1-\alpha}{\alpha-\beta}[\alpha^{m-2}(1+\alpha-2\beta) \\ \quad -\beta^{m-2}(1-\beta)] & \text{if } m \geq 2 \end{cases}$$
$$(B-2)$$

The total absorption change after m flashes is

$$\sum_{l=1}^{m} \Delta A_l^{550} = -[RC]\epsilon_{red-ox}^{550}$$
$$\times \left\{3 - \frac{(1+\alpha-2\beta)\alpha^{m-1}-(1-\alpha)\beta^{m-1}}{\alpha-\beta}\right\}. \qquad (B-3)$$

After a large number of flashes (i.e., as $m \to \infty$) the total absorption change is

$$\sum_{l=1}^{\infty} \Delta A_l^{550} = -3[RC]\epsilon_{red-ox}^{550} \qquad (B-4)$$

i.e., three Cyt c^{2+} are oxidized per reaction center.

Appendix C. Semiquinone absorption after successive flashes

The change in semiquinone absorption after successive flashes is most conveniently measured at 450 nm (see Figs. 3a and b). The change in absorption after the mth flash is defined by

$$\Delta A_m^{450} = \sum_{l=1}^{m} \Delta A_l^{450} - \sum_{l=1}^{m-1} \Delta A_l^{450}, \qquad (C-1)$$

where the total absorption after the mth flash,

$$\sum_{l=1}^{m} \Delta A_l^{450}$$

is found by summing the contributions from the individual states present after each flash (see Fig.

1), i.e.,

$$\sum_{l=1}^{m} \Delta A_l^{450} = [Q_A^- Q_B]_m \epsilon_{A^-B}^{450} + [Q_A Q_B^-]_m \epsilon_{AB}^{450}$$

$$+ [Q_A^- Q_B^-]_m \epsilon_{A^-B^-}^{450} + [Q_A^- Q_B^{2-}]_m \epsilon_{A^-B^{2-}}^{450}. \quad (C-2)$$

The extinction coefficients $\epsilon_{A^-B}^{450}$, ϵ_{AB}^{450}, $\epsilon_{A^-B^-}^{450}$ and $\epsilon_{A^-B^2}^{450}$ refer to the states $Q_A^- Q_B$, $Q_A Q_B^-$, $Q_A^- Q_B^-$ and $Q_A^- Q_B^{2-}$, respectively.

The exact expressions for the absorption changes after the first two flashes are given in the text (see Eqns. 7b and 8b) and were used to determine β (see Eqn. 11). The expressions for the absorption changes after subsequent flashes are algebraically unwieldy; the changes can be estimated, however, using the approximations

$$\epsilon_{AB}^{450} = \epsilon_{A^-B^{2-}}^{450} = \epsilon_{A^-B}^{450} \text{ and } \epsilon_{A^-B^-}^{450} = 2\epsilon_{A^-B}^{450}. \quad (C-3)$$

These approximations are valid to within approx. 20% (see Table II). The total semiquinone absorption is given by (Eqns. C-2 and C-3):

$$\sum_{l=1}^{m} \Delta A_l^{450} = \left\{ [Q_A^- Q_B]_m + [Q_A Q_B^-]_m + 2[Q_A^- Q_B^-]_m \right.$$

$$+ \left. [Q_A^- Q_B^{2-}]_m \right\} \epsilon_{A^-B}^{450}. \quad (C-4)$$

Substituting Eqns. A-4b, A-4c, A-4d and A-4f, this becomes

$$\sum_{l=1}^{m} \Delta A_l^{450} = [RC]\epsilon_{A^-B}^{450} \left\{ 1 - (1-2\beta)(1-\alpha)\frac{\alpha^{m-1} - \beta^{m-1}}{\alpha - \beta} \right\}. \quad (C-5)$$

The change in absorption after the m th flash ($m \geqslant 2$) is found by combining Eqns. C-1 and C-5, i.e.,

$$\Delta A_m^{450} = [RC]\epsilon_{A^-B}^{450}(1-2\beta)$$

$$\times (1-\alpha)\frac{(1-\alpha)\alpha^{m-2} - (1-\beta)\beta^{m-2}}{\alpha - \beta}. \quad (C-6)$$

Note that the sign of ΔA_m^{450} changes when the direction of the $Q_A^- Q_B^-$ to $Q_A Q_B^{2-}$ equilibrium changes (i.e., for $\beta = 0.5$).

Appendix D. The reduction of D^+ by Cyt c^{2+}

In the text we made simplifying assumption that for $[RC] = [Cyt \ c^{2+}]_0$, all donors (D^+) will be reduced by Cyt c^{2+} after a single saturating flash. In this appendix we discuss the validity of this assumption. The extent of reduction of D^+ by Cyt c^{2+} depends on the free-energy difference between the D/D^+ and Cyt $c^{2+}/Cyt \ c^{3+}$ redox couples and on the reaction rate, k_{cyt}, between Cyt c^{2+} and D^+ relative to the charge recombination rate of D^+ with Q_B^- (i.e., $k_{D^+ \to D}^{obs \ (1)}$). The free energy for the D/D^+ and Cyt $c^{2+}/Cyt \ c^{3+}$ redox couples is given by

$$G_{D/D^+}^{redox} = G_{D/D^+}^0 - kT \ln \frac{[D^+]}{[D]} \quad (D-1a)$$

$$= G_{D/D^+}^0 - kT \ln \frac{[RC] - [D]}{[D]} \quad (D-1b)$$

and

$$G_{c^{2+}/c^{3+}}^{redox} = G_{c^{2+}/c^{3+}}^0 - kT \ln \frac{[Cyt \ c^{3+}]}{[Cyt \ c^{2+}]} \quad (D-2a)$$

$$= G_{c^{2+}/c^{3+}}^0 - kT \ln \frac{[Cyt \ c^{3+}]}{[Cyt \ c^{2+}]_0 - [Cyt \ c^{3+}]}. \quad (D-2b)$$

where the initial population of cytochrome c was assumed to be completely reduced.

We focus our analysis on the case $k_{cyt} \gg k_{D^+ \to D}^{obs \ (1)}$. In this limit the redox couples D/D^+ and Cyt $c^{2+}/Cyt \ c^{3+}$ are in equilibrium after a flash, i.e., $G_{D/D^+}^{redox} = G_{c^{2+}/c^{3+}}^{redox}$. Furthermore; the increase in Cyt c^{3+} concentration is equal to the concentration of the oxidized donor, i.e., $[Cyt \ c^{3+}] = [D]$. With these conditions one finds from Eqns. D-1b and D-2b the fraction of reaction centers that are reduced by Cyt c^{2+}, i.e., $[D]/[RC]$,

$$\left(1 - \frac{[D]}{[RC]}\right)\left(\frac{[Cyt \ c^{2+}]_0}{[RC]} - \frac{[D]}{[RC]}\right) = \left(\frac{[D]}{[RC]}\right)^2$$

$$\times \exp\left\{ -\left(G_{c^{2+}/c^{3+}}^0 - G_{D/D^+}^0\right)/kT \right\}. \quad (D-3)$$

The first term in brackets on the left represents the fraction of reaction centers that are not reduced by Cyt c^{2+} after a first flash; the second term represents the relative concentration of Cyt c^{2+} remain-

ing after the flash. In the limit $G^0_{c^{2+}/c^{3+}} - G^0_{D/D^+} \gg kT$, the reduction of D^+ by Cyt c^{2+} occurs to completion; i.e., $[D]/[RC] = 1$ for the initial condition $[\text{Cyt } c^{2+}]_0 \geqslant [RC]$.

The reported free energies for the D/D^+ and Cyt $c^{2+}/\text{Cyt } c^{3+}$ redox couples are $G^0_{D/D^+} = -440$ meV [47,48] and $G^0_{c^{2+}/c^{3+}} = -260$ meV (pH 8) [49]. For the initial condition $[\text{Cyt } c^{2+}]_0 = [RC]$, one finds from Eqn. D-3 (at $T = 21°C$) the value $[D]/[RC] = 0.97$, i.e., 97% of the reaction centers will be reduced by Cyt c^{2+} after a flash.

References

1 Crofts, A.R. and Wraight, C.A. (1983) Biochim. Biophys. Acta 726, 149–185

2 Ort, D.R. and Melandri, B.A. (1982) in Photosynthesis. Energy Conversion by Plants and Bacteria (Govindjee, ed.), pp. 537–587, Academic Press, New York

3 Feher, G. and Okamura, M.Y. (1978) in The Photosynthetic Bacteria (Clayton, R.K. and Sistrom, W.R., eds.), pp. 349–386, Plenum Press, New York

4 Okamura, M.Y., Feher, G. and Nelson, N. (1982) in Photosynthesis. Energy Conversion by Plants and Bacteria (Govindjee, ed.), pp. 195–272, Academic Press, New York

5 Parson, W.W. and Ke, B. (1982) in Photosynthesis: Energy Conversion by Plants and Bacteria (Govindjee, ed.), pp. 331–385, Academic, New York

6 Verméglio, A. (1977) Biochim. Biophys. Acta 459, 516–524

7 Wraight, C.A. (1977) Biochim. Biophys. Acta 459, 525–531

8 Kleinfeld, D., Abresch, E.C., Okamura, M.Y. and Feher, G. (1984) Biochim. Biophys. Acta 765, 406–409.

9 Wraight, C.A. (1982) in Function of Quinones in Energy Conserving Systems (Trumpower, B.L. ed.), pp. 181–197, Academic Press, New York

10 Kleinfeld, D., Okamura, M.Y. and Feher, G. (1984) Biochim. Biophys. Acta 766, 126–140

11 Kleinfeld, D., Okamura, M.Y. and Feher, G. (1982) Biophys. J. (Abstr.) 37, 110a

12 Margoliash, E. and Frohwirt, N. (1959) Biochem. J. 71, 570–572

13 Straley, S.C., Parson, W.W., Mauzerall, D.C. and Clayton, R.C. (1973) Biochim. Biophys. Acta 305, 597–609

14 Okamura, M.Y., Debus, R.J., Kleinfeld, D. and Feher, G. (1982) in Function of Quinones in Energy Conserving Systems (Trumpower, B.L. ed.), pp. 299–317, Academic Press, New York

15 Parson, W.W. (1969) Biochim. Biophys. Acta 189, 384–396

16 Verméglio, A. and Clayton, R.K. (1977) Biochim. Biophys. Acta 461, 159–165

17 Morrison, L.E., Schelhorn, J.E., Cotton, T.M., Bering, C.L. and Loach, P.A. (1982) in Function of Quinones in Energy Conserving Systems (Trumpower, B.L. ed.), pp. 35–58, Academic Press, New York

18 Prince, R.C., Cogdell, R.J. and Crofts, A.R. (1974) Biochim. Biophys. Acta 347, 1–13

19 Wraight, C.A. and Stein, R.R. (1980) FEBS Lett. 113, 73–77

20 Verméglio, A., Martinet, T., Clayton, R.K. (1980) Proc. Natl. Acad. Sci. USA 77, 1809–1813

21 Okamura, M.Y., Isaacson, R.A. and Feher, G. (1975) Proc. Natl. Acad. Sci. USA 72, 3491–3495

22 Bensasson, R. and Land, E.J. (1973) Biochim. Biophys. Acta 325, 175–181

23 Wraight, C.A. (1979) Biochim. Biophys. Acta 548, 309–327

24 Verméglio, A. (1982) in Function of Quinones in Energy Conserving Systems (Trumpower, B.L. ed.), pp. 169–180, Academic Press, New York

25 Butler, W.F., Johnston, D.C., Shore, H.B., Fredkin, D.R., Okamura, M.Y. and Feher, G. (1980) Biophys. J. 32, 967–992

26 Van Gelder, B.F. and Slater, E.C. (1962) Biochim. Biophys. Acta 58, 593–595

27 Yonetani, T. (1965) J. Biol. Chem. 240, 4509–4514

28 Prince, R.C. and Dutton, P.L. (1976) Arch. Biochem. Biophys. 172, 329–334

29 Rutherford, A.W. and Evans, M.C.W. (1980) FEBS Lett. 110, 257–261

30 Wraight, C.A. (1981) Isr. J. Chem. 21, 348–354

31 Bouges-Bocquet, B. (1975) in Proceedings of the 3rd International Congress on Photosynthesis (Avron, M., ed.), pp. 579–588, Elsevier, Amsterdam

32 Van Best, J.A. and Duysens, L.N.M. (1975) Biochim. Biophys. Acta 408, 154–163

33 Diner, B.A. (1977) Biochim. Biophys. Acta 460, 247–258

34 Bowes, J.M. and Crofts, A.R. (1980) Biochim. Biophys. Acta 590, 373–384

35 Dutton, P.L. (1978) Methods Enzymol. 54, 411–435

36 Cogdell, R.J., Prince, R.C. and Crofts, A.R. (1973) FEBS Lett. 35, 204–208

37 Wraight, C.A., Cogdell, R.J. and Clayton, R.K. (1975) Biochim. Biophys. Acta 396, 242–249

38 Marinetti, T. (1984) Biophys J. (Abstr.) 45, 217a

39 Maróti, P. and Wraight, C.A. (1985) Biophys. J. (Abstr.) 47, 5a

40 Jackson, J.B. and Dutton, P.L. (1973) Biochim. Biophys. Acta 325, 102–113

41 Packham, N,K., Dutton, P.L. and Mueller, P. (1982) Biophys. J. 37, 465–473

42 Blatt, Y., Gopher, A., Montal, M. and Feher, G. (1983) Biophys. J. (Abstr.) 41, 121a

43 Feher, G. and Okamura, M.Y. (1984) in Advances in Photosynthesis Research (Sybesma, C., ed.), Vol II, pp. 155–164, Martinus Nijhoff/Dr. W. Junk Publishers, Dordrecht, The Netherlands

44 Gunner, M.R., Tiede, D.M., Prince, R.C. and Dutton, P.L. (1982) in Function of Quinones in Energy Conserving Systems (Trumpower, B.L. ed.) Academic Press, New York, pp. 265–269

45 Gopher, A., Blatt, Y., Schönfeld, M., Okamura, M.Y., Feher, G. and Montal, M. (1985) Biophys. J. 48, 311–320

46 Diner, B.A., Schenck, C.C. and de Vitry, C. (1984) Biochim. Biophys. Acta 766, 9–20

47 Dutton, P.L. and Jackson, J.B. (1972) Eur. J. Biochem. 30, 495–510

48 Jackson, J.B., Cogdell, R.J. and Crofts, A.R. (1973) Biochim. Biophys. Acta 292, 218–225

49 Clark, W.M. (1960) Oxidation-Reduction Potentials of Organic Systems, pp. 450–456, Robert E. Krieger, New York

50 Robinson, H.H. and Crofts, A.R. (1983) FEBS Lett. 153, 221–226

51 Arata, H. and Parson, W.W. (1981) Biochim. Biophys. Acta 638, 201–209.